Biointerface Research in Applied Chemistry

Electrospun carbon nanofiber-based electrochemical biosensor for the detection of hepatitis B virus

Alireza Dehghan Niri[1], Reza Faridi-Majidi[1], Reza Saber[1], Masood Khosravani[1], Mahdi Adabi[1, *]

[1]Department of Medical Nanotechnology, School of Advanced Technologies in Medicine, Tehran University of Medical Sciences, Iran

*corresponding author e-mail address:*madabi@tums.ac.ir*

ABSTRACT

The purpose of this work was to design the electrochemical DNA biosensor based on carbon nanofibers (CNFs) for detecting hepatitis B virus (HBV). The CNFs, due to high conductivity and surface-to-volume ratio, was known as an effective material in the electrochemical biosensor. In this work, we directly used electrospun CNF as the electrode. CNF electrode was modified with electropolymerized glutamic acid (Glu). Then, the probe DNA (pDNA) was conjugated to Glu modified CNFs electrode. The surface morphology of CNFs and Glu modified CNFs were characterized via scanning electron microscopy (SEM). Electropolymerized Glu on the surface of CNF electrode was characterized by Fourier transform infrared spectroscopy (FTIR) as well. The cyclic voltammetry (CV) was used to monitor the target DNA (tDNA). The tDNA was quantified at a linear range from 1×10^{-12} to 1×10^{-6} M with a detection limit of 1.58×10^{-12} M. This electrochemical HBV biosensor had good stability, repeatability, and selectivity for distinguishing complementary DNA from non-complementary and mis-matched DNA sequences.

Keywords: *Biosensor, Nanofiber, Electrospinning, Carbon.*

1. INTRODUCTION

The liver is one of the essential organs in the body for human life to perform different tasks[1]. Four important functions of the liver are to process nutrient, remove toxins from the body, build proteins and make bile[2]. Hepatitis B virus (HBV) is considered as a causative agent of viral hepatitis and a public health problem of worldwide with a clinical consequence such as liver cirrhosis and hepatocellular carcinoma[3]. HBV due to mutation of structural genes can have fast proliferation and tolerance to antiviral drugs[4]. Therefore, it is important to know about the presence or loss of HBV DNA in blood serum via molecular hybridization assays during and after the therapy process.

A rapid, inexpensive, simple, sensitive and selective DNA analysis has been attracted great attention in clinical and molecular diagnostics especially for the detections with low concentrations of pathogenic agents such as HBV. To date, many methods have been developed for DNA detection such as surface plasmon resonance[5], surface-enhanced Raman scattering[6], fluorescence[7], and electrochemical[6, 8] techniques. Among these, the electrochemical method has several advantages such as high sensitivity, simplicity, rapidness, and low cost[8]. In electrochemical DNA hybridization biosensors, different electrodes like gold, platinum and carbon paste electrode have been used[9]. Metal electrodes have some disadvantages like the formation of oxide layers on the surface of the electrode, leads to a decrease in electron transfer and analytical signal[10]. In addition,

using oil in carbon paste electrodes decrease the conductivity of electrode[11]. In this work, we used electrospinning method to prepare an electrospun CNF electrode which is loss of oil and oxide layer. The electrospinning device composes of a nozzle, a collector covered with aluminum foil and a high voltage power source. The potential difference between nozzle and collector causes a stretched thin jet from polymeric solution toward the collector and the formation of ultrafine nanofibers on the collector[12-14].

To date, several biosensors were designed to detect HBV. For example; Shakoori *et al*[15] used a gold electrode modified with nano-gold rod to detect HBV DNA with a detection limit of 2.0×10^{-12}. Li *et al*[16] used metalloimmunoassay paper for the detection of HBV DNA with a detection limit of 85.0×10^{-12}. Wang *et al*[17] used single walled carbon nanotube array coated with gold nanoparticles to measure the DNA sequences of HBV with a detection limit of 0.1×10^{-12}. In this work, we designed an electrochemical HBV biosensor via the electrospun CNF electrode based polyacrylonitrile (PAN) which is directly used as transducer without any oil and oxide layer. Glu was then electropolymerized on the surface of the electrospun CNF electrode to be conjugated to pDNA. In the end, tDNA was hybridized to pDNA/Glu modified CNF electrode. In addition, linear range, detection limit, stability, repeatability and selectivity were investigated.

2. MATERIALS AND METHODS

2.1. Materials.

polyacrylonitrile (PAN) was purchased from Polyacryl company (Iran) with a molecular weight of 150,000 g·mol⁻¹. Glutamic acid (Glu) was received from Carlo Erba company.

Dimethylformamide(DMF), and N-Hydroxysuccinimide (NHS) and potassium ferricyanide were bought from Merck company. 1-(3-dimethylaminopropyl)-3-ethylcarbodiimide (EDC) was bought from Alfa Aesar. Sodium phosphate dibasic and potassium

phosphate monobasic and potassium chloride were from Sigma-Aldrich company. Phosphate buffer solutions (PBS) were prepared by 0.1 M Na_2HPO_4 and 0.1M KH_2PO_4.

The oligonucleotide sequence was investigated by Basic Local Alignment Search Tool (BLAST) to have the least similarity to the human serum genome. The DNA oligomer sequences designed for hepatitis B detection were as follows:

probe DNA (pDNA): 5′-$NH_2(CH_2)_6$TAC CGT CCC CTT CTT CAT CTG CCG T- 3′

target DNA (tDNA): 5′ -ACG GCA GAT GAA GAA GGG GAC GGT A - 3′

one-point mismatch DNA: 5′- ACG CCA GAT GAA GAA GGG GAC GGT A-3′

non-complementary DNA: 5′- TAC CGT CCC CTT CTT CAT CTG CCG T - 3′

The oligonucleotide solutions were prepared in PBS (100 mM, pH =7.4). All solutions were prepared by ultra-pure water.

2.2. Preparation of CNF electrode.

The CNFs were prepared according to our previous work[18]. Briefly, PAN polymer (with the concentration of 8 wt%) was dissolved in a mixture of DMF and acetone at 8 to 2 ratio with magnetic stirring at 50 °C for 8 hours. The PAN solution was extruded through a 10 mL plastic syringe fitted with an 18-gauge needle as nozzle and electrospun by Electroris (Fanavaran Nano Meghyas Ltd., Co., Tehran, Iran) at a flow rate of 1.2 ml/h with an applied voltage of 12.00 kV at room temperature. The distance between the tip-to-collector and rotating drum were also 12 cm and 150 rpm, respectively. The electrospun PAN nanofibers were separated from aluminum foil wrapped collector and dried at room temperature. Then, the morphology and diameter of PAN nanofibers were characterized (Fig. 1a) by SEM. Afterward, the electrospun PAN nanofibers were put into a tube furnace (Azar, TF5/25–1720) and stabilized in air atmosphere for 4 hours with a heating rate 1.5 °C min^{-1} at 290 °C. Then, stabilized nanofibers were carbonized for 1 hour in a nitrogen atmosphere with a heating rate of 4 °C min^{-1} at 1000 °C. The morphology and diameter of stabilized and carbonized nanofibers (Fig. 1b and c) were characterized by SEM. Inthe end, electrospun CNFs were spherically cut at a size of 5 mm and inserted with a metal wire to have the electrical contact.

2.3. Preparation of Glu modified CNFs electrode.

The Glu modified CNF electrode was fabricated using electropolymerization of Glu on the surface of CNF electrode in a solution which contains 0.01 M Glu and 0.1 M PBS (pH 7.0) in the potential range from −0.5 to 2.0 V at a scan rate of 100 mV.s^{-1} with scan number of 2. After electropolymerization, the Glu modified CNFs electrode was carefully washed with ultrapure water to remove residual monomer solution. The morphology of Glu modified CNF nanofibers (Fig. 1d) were characterized by SEM. In addition, functional groups of Glu investigated by FTIR.

2.4. Immobilization of pDNA on the Glu modified CNF electrode and hybridization tDNA to pDNA.

The pDNA with a terminal amino group was covalently immobilized onto Glu modified CNF electrode. Carboxylic groups available in Glu were activated via interaction with an aqueous solution containing 8.0 mM EDC and 5.0 mM NHS for 1 hour. The pDNA was subsequently placed on the Glu modified CNF electrode by conjugation between a carboxylic group of Glu and the terminal amine group of pDNA to form amide bonds. After pDNA immobilization, 10 μL tDNA was poured on the pDNA/Glu modified CNF electrode and dried in room temperature to be hybridized to pDNA.

2.5. Characterization.

The diameter and morphology of PAN and CNFs nanofibers were performed by SEM (Philips XL-30) at an accelerating voltage of 20.0 kV after sputtering gold on the pieces of PAN and CNF. The mean diameter of 50 nanofibers was calculated by SemAfore (4.01 demo, JEOL, Finland) software.

X-ray diffraction (XRD) of CuKα radiation (λ = 1.54056 Å) was carried out using a Philips Xpert instrument operating at 40 kV and 30 mA conditions with at a step size of 0.08°/s over the 2θ range of 10–80° at room temperature to investigate the crystalline structure of CNFs.

Raman spectra were performed with 25 mW power laser and 758 nm laser wavenumber and resolution about 3.0 cm^{-1} (model: sentera (2009) Bruker (Germany)). The spectra were recorded at room temperature. The measurement was taken at three various spots on the sample to realize the homogenous nature of the CNFs. FTIR spectra were collected in a Nicolet iS10 spectrometer (USA) over a range of 4000 cm^{-1} to 400 cm^{-1} after mixing with KBr powder to determine carboxylic groups of electropolymerized Glu on CNF.

All electrochemical experiments were obtained by μStat 400 potentiostat/galvanostat (DropSens, Spain). Ag/AgCl and platinum wire electrodes were applied as the reference and auxiliary electrodes, respectively.

3. RESULTS

3.1. The effect of electrospinning parameters on PAN nanofibers.

Table 1 summarizes several electrospinning parameters which affect morphology and diameter of PAN nanofibers as a precursor of CNFs. The function of concentration as an effective factor affects the diameter of PAN nanofibers. In this experiment, we applied three different concentrations including 6.00, 8.00 and 10.00 wt% whilst other parameters were constant. The results indicated that the diameter of PAN nanofibers decreased from 239 to 116 nm as the PAN concentration reduced from 10.00 to 6.00 wt%. The reason for this finding could be due to the viscosity of the solution. In low viscous solution, thin nanofibers form due to increase in the mobility and entanglement of the polymer chain. Besides, the beaded PAN nanofibers appeared in low viscous solution (6.00 wt%) whereas uniform nanofibers formed in a concentration of 8.00 and 10.00 wt% solution. Another effective parameter on the diameter of nanofibers and morphology was the ratio of solvents. In this experiment, the different ratios of solvents were applied for the solution with 8.00 wt% concentration whilst other parameters were constant. We used two different solvent

including DMF and acetone. When the ratio of acetone increases from 0 to 4 (according to table 1) in solution, the diameter of non-beaded nanofibers enhanced from 70 to 257 nm. In addition, the higher amount of acetone in solution resulted in the beaded nanofibers or beads without any nanofibers.

The effects of tip to collector distance on the diameter of nanofibers are also investigated. In 8.00 wt% concentration, the distance as a variable parameter enhanced from 8 to 16 cm whereas the other parameters were constant. According to table1, the diameter of nanofibers decreased from 226 to 169 nm as tip to collector distance increased. The decrease in the diameter of nanofibers may be due to the formation of two or several jet originated from a jet which can lead to the formation of thinner nanofibers.
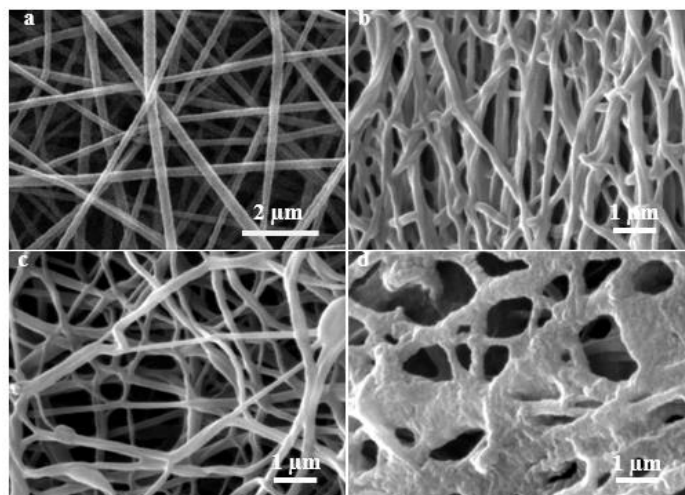
Fig. 1. morphology of (a) PAN, (b) stabilized PAN, and (c) CNF prepared with 8.00 wt% concentration; (d) Electropolymerized glutamic acid on CNF.
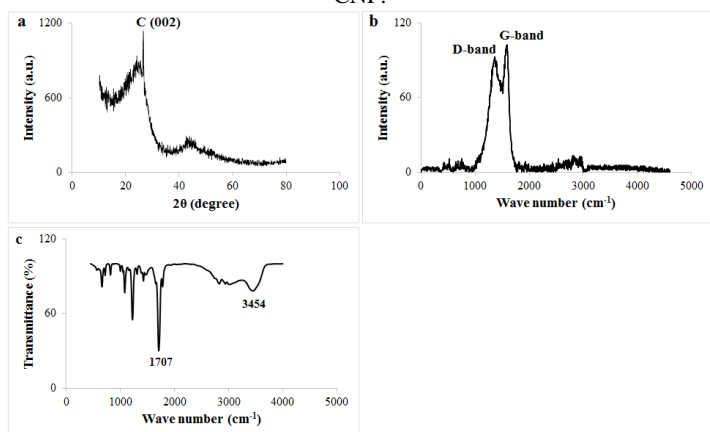
Fig. 2. (a) XRD, (b) Raman spectroscopy,and (c) FTIR curve of PAN-based CNFs.

The flow rate also affects the diameter of nanofibers. In 8.00 wt% concentration, the flow rate as a variable factor enhanced from 0.5 to 2.0 ml/h whilst the other factors were constant. The mean diameter of nanofibers enhanced by increasing flow rate from 0.5 to 1.2 ml/h whereas the diameter of nanofibers was loss of significant change as flow rate increased from 1.2 to 2.0 ml/h. The reason may be related to this finding that by increasing flow rate, the higher amounts of polymer solution are gathered apex tip of nozzle which can form nanofibers with a larger diameter.

The effect of voltage on the diameter of nanofibers is shown in table1. In 8.00 wt% concentration, applied voltage as a variable parameter enhanced from 8 to 16 kV whereas the other parameters

were constant. The mean diameter of nanofibers increased from about 168 to 282 nm with enhancement in the applied voltage. This finding can be described that by increasing the applied voltage, the polymer solution moves faster from tip to collector, places on the collector in less time and finally leads to nanofibers with a larger diameter.

3.2. Morphology and structure of nanofibers.

In this experiment, PAN nanofibers with 8.00 wt% concentration were chosen for the fabrication of CNFs. The diameter of CNFs decreased compared to PAN nanofibers because of heat treatment, resulting in the remove of non-carbon elements in the form of different gases such as NH_3, HCN and H_2O, and consequently shrinkage of nanofibers.

3.3. XRD and Raman spectroscopy analysis of CNFs and FTIR of Glu modified CNFs.

XRD pattern and Raman spectroscopy obtained from electrospun CNFs is showed in Fig. 2a. The results for XRD (Fig. 2a) exhibit that diffraction peak is around the $2\theta \sim 26$ which indicate to the crystallographic plane of graphic layer. In addition, the results for Raman spectroscopy (Fig. 2b) demonstrate two peaks about wavenumber of 1366 cm^{-1} and 1587 cm^{-1} which are related to turbostratic carbon and graphitic structure, respectively. For confirming the placement of Glu on the surface of CNFs, FTIR pattern of Glu modified CNFs was investigated. As seen in Fig. 2c, there are two peaks in the wavenumber of 1707 and 3454 cm^{-1} which are related to carbonyl and hydroxyl groups of Glu.
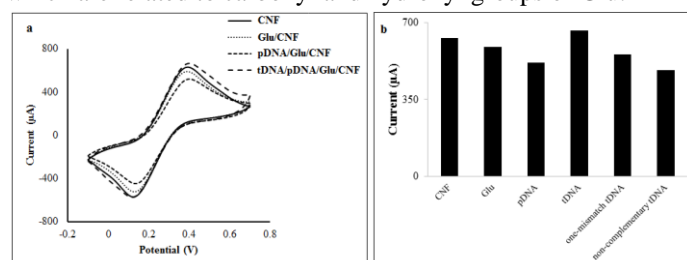
Fig. 3. cyclic voltametric behavior of (a) bare CNF electrode, Glu modified CNF electrode, pDNA/Glu modified CNF electrode and tDNA/pDNA/Glu modified CNF electrode, (b) bare CNF electrode, Glu modified CNF electrode, pDNA/Glu modified CNF electrode, tDNA/pDNA/Glu modified CNF electrode, one-mismatch tDNA/pDNA/Glu modified CNF electrode and non-complementary/pDNA/Glu modified CNF electrode for 5 mM $K_3Fe(CN)_6$ in 0.1 M PBS at pH 7 and scan rate 100 mV·s^{-1}

3.4. Cyclic voltammetric behavior of the modified CNF electrode.

In this work, we directly used CNFs as working electrode. In Fig. 3, the cyclic voltammetric behavior of the bare CNF electrode is exhibited. In our previous work[18], we explained that the current of the CNFs depends on the diameter and morphology of CNFs. Decreasing in both the diameter of CNFs and the number of beads results in the higher amount of current. Therefore, we chose 8.00 wt% concentration of PAN solution for the preparation of CNFs which had better performance as a working electrode for electron transfer due to low diameter and bead. Afterward, cyclic voltammogram of Glu modified CNF electrode was investigated. It is observed that the voltametric response of $[Fe(CN)_6]^{3-}$ redox for Glu modified CNF electrode decreased compared to bare CNF one. The reduced current response of Glu modified CNF electrode is due to the placement of Glu on the surface of CNF electrode as Glu makes a barrier between the surface of Glu modified CNF

electrode and electroactive species for electron transfer. In addition, Glu has carboxylic groups, resulting in the repulsion of $[Fe(CN)_6]^{3-}$ and consequently less current in a cyclic voltammogram. Then cyclic voltammogram of modified CNF electrode after conjugation of pDNA to Glu modified CNF electrodewas also investigated. The results exhibit that current for pDNA/Glu modified CNF electrode decreased compared to Glu modified CNF one which indicates to immobilization of the pDNA on the surface of Glu modified CNF electrode. pDNA has amine groups which can be conjugated to carboxylic groups of Glu. This conjugation provides more barrier between the surface of Glu modified CNF electrode and electroactive species for electron transfer. Besides, pDNA has negatively-charged phosphate backbone which repel$[Fe(CN)_6]^{3-}$ and leads to a decrease in current. As seen in curve related to tDNA/pDNA/Glu modified CNF electrode, the current increased after hybridization of tDNA to pDNA. This increase may be due to the release of pDNA and Glu from the surface of CNF electrode after attachment of tDNA to pDNA/Glu modified CNF electrode. Therefore, the barrier between the surface of CNF electrode and electroactive species decreases, leading to an increase in current.

The selectivity of HBV biosensor was also investigated via cyclic voltametric behavior of $[Fe(CN)_6]^{3-}$. In this experiment, three tDNA including complementary, one-point-mismatch and non-complementary tDNA for pDNA were selected. According to Fig. 3b, the highest and lowest amount of current was for complementary tDNA and non-complementary tDNA, respectively. The highest amount of current indicates to hybridization of complementary tDNA to pDNA and the lowest amount of current exhibit lack of hybridization of non-complementary tDNA to pDNA. In addition, the amount of

current for one-pointed-mismatch tDNA decreased by about 13% compared to complementary tDNA.
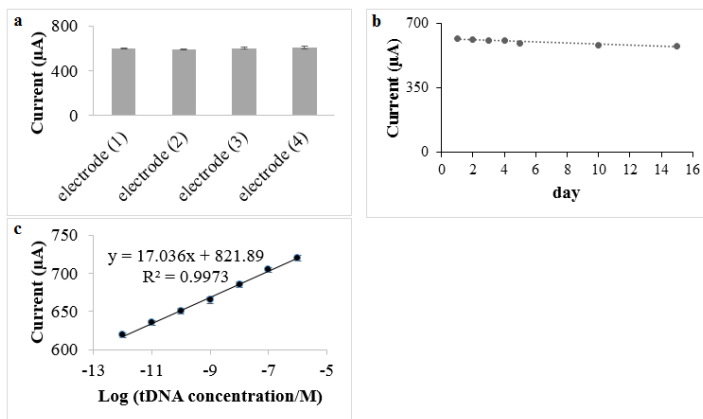
Fig. 4. (a) repeatability and (b) stability of the biosensor; (c) relationship of current change to tDNA concentration.

To investigate the repeatability of HBV biosensor, four modified CNFs electrodes were prepared and each electrode was repeated three times. As shown in Fig. 4a, the results had good repeatability for all electrodes. For the stability of HBV biosensor, the modified electrodes were investigated for 15 days. The results (Fig. 4b) indicated the performance of electrodes decreased by about 6.5% during 15 days. In addition, the linear range and detection limit of the biosensor was investigated. As seen in Fig. 4c, the regression equation was y=17.036x+821.89 and R^2 was 0.9973 with the linear range of 1×10^{-12} to 1×10^{-6} M. To estimate the detection limit, the formula $3\sigma/a$ was used (where σ is the standard deviation of the blank solution and a is the slope of line) to indicate detection limit of 1.58×10^{-12} M.

Table 1. Electrospinning data for PAN nanofibers.

No	PAN concentration (wt.%)	DMF to acetone ratio	Distance between tip to collector (cm)	Flow rate (mL/h)	Voltage (kV)	Mean diameter of nanofibers (nm)	Morphology
1	8	8:2	12	1.2	12	191	nanofiber
2	6	8:2	12	1.2	12	116	beaded nanofiber
3	10	8:2	12	1.2	12	239	nanofiber
4	8	10:0	12	1.2	12	70	beaded nanofiber
5	8	6:4	12	1.2	12	257	beaded nanofiber
6	8	0:10	12	1.2	12	0	bead
7	8	8:2	12	1.2	8	168	nanofiber
8	8	8:2	12	1.2	16	282	nanofiber
9	8	8:2	8	1.2	12	226	nanofiber
10	8	8:2	16	1.2	12	169	beaded nanofiber
11	8	8:2	12	0.5	12	171	nanofiber
12	8	8:2	12	2	12	195	nanofiber
13	8	8:2	12	1.2	12	168	nanofiber
14	8	8:2	12	1.2	12	164	nanofiber

4. CONCLUSIONS

In the present study, we prepared an electrochemical DNA biosensor based on electrospun CNF mat for detecting HBV. Electrospun CNF mat was directly used as the electrode because of their high ability to electron transfer and large surface area. The results indicated that morphology and diameter of PAN nanofibers have great importance in the formation of electrospun CNFs as an electrode. The constructed biosensor had a linear range from 1.0×10^{-12} to 1.0×10^{-6} M with a detection limit of 1.58×10^{-12} M. In addition, the proposed biosensor indicated a good selectivity, stability, and repeatability. In conclusion, it is proposed that electrospun CNFs can be directly used as an electrode for the application in electrochemical biosensors.

5. REFERENCES

1. Castro, A.C.H.; França, E.G.; de Paula, L.F.; Soares, M.M.; Goulart, L.R.; Madurro, J.M.; Brito-Madurro, A.G. Preparation of genosensor for detection of specific DNA sequence of the hepatitis B virus. *Applied Surface Science* **2014,***314*, 273-279, https://doi.org/10.1016/j.apsusc.2014.06.084.

2. Chen, H.L.; Liu, D.Y.; Yang, B.; Liu, J.; Wang, G. A new hybrid method based on local fisher discriminant analysis and support vector machines for hepatitis disease diagnosis. *Expert Systems with Applications* **2011,***38*, 11796-11803, https://doi.org/10.1016/j.eswa.2011.03.066

3. Nishikawa, T.; Bellance, N.; Damm, A.; Bing, H.; Zhu, Z.; Handa, K.; Yovchev, M.I.; Sehgal, V.; Moss, T.J.; Oertel, M. A switch in the source of ATP production and a loss in capacity to perform glycolysis are hallmarks of hepatocyte failure in advance liver disease. *Journal of hepatology* **2014,***60*, 1203-1211, https://doi.org/10.1016/j.jhep.2014.02.014

4. Dondeti, M.F.; Talaat, R.M.; El-Shenawy, S.Z.; Khamiss, O.A. Transforming growth factor (TGF-β1) gene polymorphisms in Egyptian patients with hepatitis B virus infection. *Meta Gene* **2017,***13*, 5-12, https://doi.org/10.1016/j.mgene.2017.03.005.

5. Ma, Z.; Tian, L.; Wang, T.; Wang, C. Optical DNA detection based on gold nanorods aggregation. *Analytica chimica acta* **2010,***673*, 179-184, https://doi.org/10.1016/j.aca.2010.05.036.

6. Dong, X.Y.; Mi, X.N.; Zhang, L.; Liang, T.M.; Xu, J.J.; Chen, H.Y. DNAzyme-functionalized Pt nanoparticles/carbon nanotubes for amplified sandwich electrochemical DNA analysis. *Biosensors and Bioelectronics* **2012,***38*, 337-341, https://doi.org/10.1016/j.bios.2012.06.015.

7. Li, F.; Huang, Y.; Yang, Q.; Zhong, Z.; Li, D.; Wang, L.; Song, S.; Fan, C. A graphene-enhanced molecular beacon for homogeneous DNA detection. *Nanoscale* **2010,***2*, 1021-1026, http://dx.doi.org/10.1039/b9nr00401g.

8. Han, X.; Fang, X.; Shi, A.; Wang, J.; Zhang, Y. An electrochemical DNA biosensor based on gold nanorods decorated graphene oxide sheets for sensing platform. *Analytical biochemistry* **2013,***443*, 117-123, https://doi.org/10.1016/j.ab.2013.08.027.

9. Adabi, M.; Saber, R.; Naghibzadeh, M.; Faridbod, F.; Faridi-Majidi, R. Parameters affecting carbon nanofiber electrodes for measurement of cathodic current in electrochemical sensors: an investigation using artificial neural network. *RSC Advances* **2015,***5*, 81243-81252, http://dx.doi.org/10.1039/c5ra15541j.

10. Uslu, B.; Ozkan, S.A. Solid electrodes in electroanalytical chemistry: present applications and prospects for high throughput screening of drug compounds. *Combinatorial chemistry & high throughput screening* **2007,***10*, 495-513, http://dx.doi.org/10.2174/138620707782152425.

11. Xuyen, N.T.; Ra, E.J.; Geng, H.Z.; Kim, K.K.; An, K.H.; Lee, Y.H. Enhancement of conductivity by diameter control of polyimide-based electrospun carbon nanofibers. *The Journal of Physical Chemistry B* **2007,***111*, 11350-11353, https://doi.org/10.1021/jp075541q.

12. Esnaashari, S.S.; Naghibzadeh, M.; Adabi, M.; Faridi Majidi, R. Evaluation of the Effective Electrospinning Parameters Controlling Kefiran Nanofibers Diameter Using Modelling Artificial Neural Networks. *Nanomedicine Research Journal* **2017,***2*, 239-249, https://dx.doi.org/10.22034/nmrj.2017.04.005.

13. Ketabchi, N.; Naghibzadeh, M.; Adabi, M.; Esnaashari, S. S.; Faridi-Majidi, R. Preparation and optimization of chitosan/polyethylene oxide nanofiber diameter using artificial neural networks. *Neural Computing and Applications* **2017,***28*, 3131-3143, https://doi.org/10.1007/s00521-016-2212-0.

14. Samadian, H.; Zakariaee, S.S.; Adabi, M.; Mobasheri, H.; Azami, M.; Faridi-Majidi, R. Effective parameters on conductivity of mineralized carbon nanofibers: an investigation using artificial neural networks. *RSC Advances* **2016,***6*, 111908-111918, http://dx.doi.org/10.1039/C6RA21596C.

15. Shakoori, Z.; Salimian, S.; Kharrazi, S.; Adabi, M.; Saber, R. Electrochemical DNA biosensor based on gold nanorods for detecting hepatitis B virus. *Analytical and bioanalytical chemistry* **2015,***407*, 455-461, https://doi.org/10.1007/s00216-014-8303-9.

16. Li, X.; Scida, K.; Crooks, R.M. Detection of hepatitis B virus DNA with a paper electrochemical sensor. *Analytical chemistry* **2015,***87*, 9009-9015, https://doi.org/10.1021/acs.analchem.5b02210.

17. Wang, S.; Li, L.; Jin, H.; Yang, T.; Bao, W.; Huang, S.; Wang, J. Electrochemical detection of hepatitis B and papilloma virus DNAs using SWCNT array coated with gold nanoparticles. *Biosensors and Bioelectronics* **2013,***41*, 205-210, https://doi.org/10.1016/j.bios.2012.08.021.

18. Adabi, M.; Saber, R.; Faridi-Majidi, R.; Faridbod, F. Performance of electrodes synthesized with polyacrylonitrile-based carbon nanofibers for application in electrochemical sensors and biosensors. *Materials science and engineering: C* **2015,***48*, 673-678, https://doi.org/10.1016/j.msec.2014.12.051.

6. ACKNOWLEDGEMENTS